Journal of Nano- and Electronic Physics
Vol. **18** No 2, 02009(6pp) (2026)

Журнал нано- та електронної фізики
Том **18** № 2, 02009(6cc) (2026)

OPEN ACCESS

REGULAR ARTICLE

Thermodynamic Modeling of Phase Composition of Si/Si Oxide Structures Obtained by Phase Separation of Nonstoichiometric Si Oxides

V. Naholenko[1,*], A. Sarikov[2,3,4,†], O. Ryzhko[1]

[1] *Anatolii Lyhun Scientific Lyceum of Kam'ianske City Council, 51925 Kam'ianske, Ukraine*
[2] *V. Lashkaryov Institute of Semiconductor Physics, National Academy of Sciences of Ukraine, 03028 Kyiv, Ukraine*
[3] *Educational Scientific Institute of High Technologies, Taras Shevchenko National University of Kyiv, 03022 Kyiv, Ukraine*
[4] *National Technical University of Ukraine "Igor Sikorsky Kyiv Polytechnic Institute", 03056 Kyiv, Ukraine*

(Received 16 November 2025; revised manuscript received 20 April 2026; published online 29 April 2026)

The article investigates the effect of annealing temperature and initial stoichiometry of Si oxide in a wide range on the phase composition of Si/SiO_x nanocomposites formed by phase separation induced by high-temperature annealing. In this study, the appearance of internal stress hindering the phase separation process, is taken into account. The equilibrium stoichiometry of the Si oxide matrix, the relative amount of Si precipitated into the Si phase and the average precipitate size as functions of the specified parameters are modelled thermodynamically. The dependence of the percolation threshold of the Si nanoinclusions on the annealing temperature is determined. The obtained results are discussed comparing the contributions from different mechanisms during phase separation into the Gibbs free energy of Si/Si oxide systems.

Keywords: Nonstoichiometric Si oxide, Phase composition, Phase separation, Si nanoparticles, Percolation threshold.

DOI: 10.21272/jnep.18(2).02009 PACS numbers: 61.43.Dq, 64.75.g, 64.75.Jk, 68.55.a

1. INTRODUCTION

Nonstoichiometric Si oxide films (SiO_x, $x < 2$) are widely used in various technological applications such as for optical coatings [1], insulating spacers [2], and protective layers of electronic devices [3]. Moreover, composite structures, in which nanosized Si (nano-Si) inclusions are dispersed within a Si oxide matrix, are proposed to use in nonvolatile memory chips [4], third-generation solar cells [5], light-emitting devices [6], and photodiodes [7].

Composite structures with nano-Si inclusions embedded in a Si oxide matrix are most commonly obtained by high-temperature annealing of SiO_x films. Such annealing induces phase transformation of the nonstoichiometric oxide, resulting in the separation of Si phase in the form of nanosized particles according to the following reaction [8]:

$$x\mathrm{SiO}_{x_0} \rightarrow x_0\mathrm{SiO}_x + (x - x_0)\mathrm{Si}, \quad x_0 < x \leq 2 \quad (1)$$

This process is driven by the smaller value of the Gibbs free energy of the phase-separated system as compared to the one of the initial nonstoichiometric Si oxide [9, 10]. At the same time, as the amount of the separated Si increases, the value of the internal stress also increases, which generally leads to incomplete separation into Si and Si oxide phases ($x < 2$ in the expression (1)) [10-13].

The main parameters defining phase composition of the formed nano-Si/Si oxide composites are the annealing temperature and the initial stoichiometry of the nonstoichiometric Si oxide. In [9], a thermodynamics theory describing equilibrium states in Si/Si oxide systems was proposed giving an insight into the mechanisms of formation of nano-Si/Si oxide composites by high-temperature annealing. Later, this theory was modified to account for the effect of internal stress on the equilibrium nano-Si/Si oxide phase composition [13]. A comprehensive thermodynamic theory of the phase separation process in nonstoichiometric Si oxides disclosing all its key aspects was presented recently [10]. At this, however, the outcomes of the mentioned theories were considered for only a limited range of initial SiO_x stoichiometries, $x_0 \geq 1$. On the other hand, the films with $x_0 < 1$ are of interest as well. In such films, the stress arising during annealing, may affect formation of interconnected Si inclusions or even completely percolated Si networks [14, 15], and this influence was not discussed earlier in the literature.

The aim of this work is to determine the effect of annealing temperature and initial SiO_x stoichiometry in a wide range on Si/Si oxide phase composition, taking into account appearance of internal stress. This aim involves calculating a number of the characteristics of Si/Si oxide systems such as the equilibrium stoichiometry of the Si oxide matrix, the relative amount of Si precipitated into the Si phase, the average size of Si nanoparticles, and the percolation threshold, which corresponds to the initial

* Correspondence e-mail: nagolenkov@gmail.com
† sarikov@isp.kiev.ua

Cite this article as: V. Naholenko et al., *J. Nano- Electron. Phys.* 18 No 2, 02009 (2026) https://doi.org/10.21272/jnep.18(2).02009

SiO_x stoichiometry at which fully interconnected Si network begins to form in result of annealing. The obtained results will enhance our understanding of the processes in nonstoichiometric Si oxides and will give a clue to developing technologies of nano-Si/Si oxide composites with tailored Si morphology for practical applications.

2. MODEL

The process of phase separation in SiO_x films is characterized by transformation of the Gibbs free energy toward its minimum value. The microstructure of the nonstoichiometric Si oxide is formed by $Si–O_ySi_{4-y}$ ($0 \le y \le 4$) tetrahedral units with a central Si atom [8, 9]. The energy state of these units is described in terms of the penalty energy $\Delta_y = \{0, 0.5, 0.51, 0.22, 0\}$ eV [16] representing energy non-equivalence of the units with different oxidation degrees y. During annealing, oxygen atoms migrate from the units with lower oxidation degrees to more oxidized ones [17]. Local disproportionation leads to a decrease in the total penalty energy of the $Si–O_ySi_{4-y}$ tetrahedral units, which is the driving force of phase separation of a nonstoichiometric Si oxide [9, 10].

The expression for the reduced Gibbs free energy of a Si/Si oxide system taking into account all the involved mechanisms has the following form [13]:

$$g'(x_0,x,T) = \\ = \frac{x_0}{1+x_0}\left\{\frac{1}{x}\sum_{y=0}^{4}\frac{4!}{(4-y)!\,y!}\left(\frac{x}{2}\right)^y\left[\frac{2-y}{2}\right]^{4-y}\Delta_y - \right. \\ - k_B(T+273)\left(\frac{2}{x}\ln\frac{2}{2-x}-\ln\frac{x}{2-x}\right) - \\ \left. - \frac{1}{x}\frac{h_e - s_E(T+273)}{N_A}\right\} + \chi(T)(x-x_0)^2 \quad (2)$$

Here, $g'(x_0, x, T)$ is the reduced (i. e., not taking into account the terms that are not functions of x, see [9] for details) Gibbs free energy per one atom of the considered system, k_B is the Boltzmann constant, h_E = 13400 J/mol is the molar crystallization enthalpy of amorphous Si [18], s_E = 3.97 eV/mol·K is the molar excess entropy of amorphous-to-crystalline transition of Si [19], and N_A is the Avogadro constant, respectively. The first contribution in the expression (2) corresponds to the penalty energy of all the $Si–O_ySi_{4-y}$ tetrahedral units. The second contribution describes the effect of configuration entropy associated with the number of possible arrangements of oxygen atoms between pairs of Si atoms in the Si oxide phase. The third contribution origins from the release of Si into the amorphous phase, which has an excess free energy as compared to the crystalline one [20]. Finally, the last term in the expression (2) describes the contribution of the internal stress to the Gibbs free energy of the Si/Si oxide system. In this term, the empirical function $\chi(T)$ has been determined as follows [13]:

$$\chi(T) = \chi_0 + \chi_1 \exp\left(\frac{\varepsilon}{k_B(T+273)}\right) \quad (3)$$

where χ_0 = – 0.52 eV/atom, χ_1 = 0.18 eV/atom and ε = 0.11 eV were determined fitting the calculated equilibrium Si oxide stoichiometries in the phase separated Si/Si oxide systems to respective experimental data [11, 13].

In accordance with the article goal, the values of the equilibrium stoichiometry index of the Si oxide matrix, the relative amount of Si precipitated into the Si phase, and the average radius of Si nanoparticles were calculated as functions of the initial SiO_x stoichiometry and annealing temperature. Moreover, the temperature dependence of the percolation threshold was calculated.

The equilibrium stoichiometry of the Si oxide matrix $x_{eq}(x_0, T)$ was calculated as the value of x in the expression (2), at which the Gibbs free energy $g'(x_0, x, T)$ has minimum value.

The relative amount of silicon precipitated into the Si phase, $r(x_0, x_{eq}, T)$, was calculated as the ratio of the quantity of Si atoms precipitated into the Si phase to the maximum possible precipitated quantity, which is achieved at complete phase separation (x = 2). Calculating these quantities gives the following expression:

$$r(x_0,x_{eq},T) = \frac{x_{eq}-x_0}{2-x_0}\times\frac{2}{x_{eq}} \quad (4)$$

For simplicity, all the Si nanoparticles were considered spherical and their radii were assumed to have the same value. The expression for the nanoparticle radius as a function of the initial Si oxide stoichiometry, the equilibrium stoichiometry of the Si oxide matrix, and the annealing temperature, $R(x_0, x_{eq}, T)$, is thus written as follows [10]:

$$R(x_0,x_{eq},T) = \left(\frac{3\Omega}{4\pi}\times\frac{x_{eq}-x_0}{x_{eq}(1+x_0)}\times\frac{C_0}{C_{incl}}\right)^{1/3} \quad (5)$$

Here, Ω = 22.9 nm^3 is the atomic volume of Si in the Si phase [21], $C_0 = 7 \times 10^{22}$ cm^{-3} is accepted to be the total atom concentration in the Si oxide phase [22], and $C_{incl} = 10^{18}$ cm^{-3} is the typical concentration of Si nanoinclusions formed in result of phase separation [23, 24], respectively.

The percolation threshold is defined here as the value of the initial stoichiometry index of the Si oxide, at which the average diameter of the formed Si nanoparticles is equal to the average distance between them (see Fig. 1b) so that a complete interconnected Si network begins to form. At the particle diameters smaller than the average interparticle distance, the particles will be isolated from each other (see Fig. 1a). When the particle diameter exceeds the average distance between the particles centers, the Si phase precipitates as a continuous network formed by interconnected nanoparticles (see Fig. 2c).

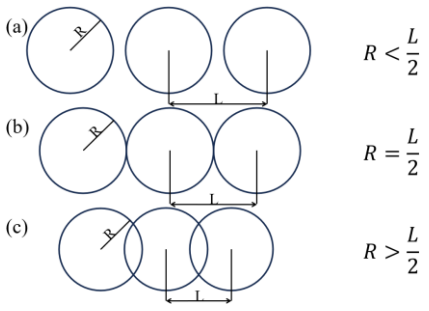

Fig. 1 – Graphical representation of the percolation threshold concept: isolated Si nanoparticles (a), percolation threshold (b), Si particles forming a continuous network (c)

3. RESULTS AND DISCUSSION

3.1 Equilibrium Stoichiometry of Si Oxide in Nano-Si/Si Oxide Composites

As demonstrated in [8-10, 13], the key mechanisms defining the equilibrium stoichiometry index of the Si oxide matrix obtained by phase separation of nonstoichiometric Si oxides are redistribution of oxygen atoms between the Si–O$_y$Si$_{4-y}$ tetrahedral units, caused by the tendency to reduce their penalty energy, and appearance of internal stress suppressing this process. Analysis of the expression (2) shows that the contribution of the internal stress to the Gibbs free energy decreases with the increase in the annealing temperature, which leads to an increase in the values of x_{eq}. This conclusion is confirmed by the Fig. 2a, in which dependences of x_{eq} versus annealing temperature for different initial SiO$_x$ stoichiometries are shown. As can be further seen from this figure, when the temperature reaches ~ 950 °C and above, the equilibrium stoichiometry index of the matrix reaches saturation at $x_{eq} \approx 2$ regardless of the initial Si oxide stoichiometry, which corresponds to almost complete phase separation. This saturation is caused by total relaxation of the internal stress and is fully consistent with numerous published experimental results (see e.g. [11, 12]).

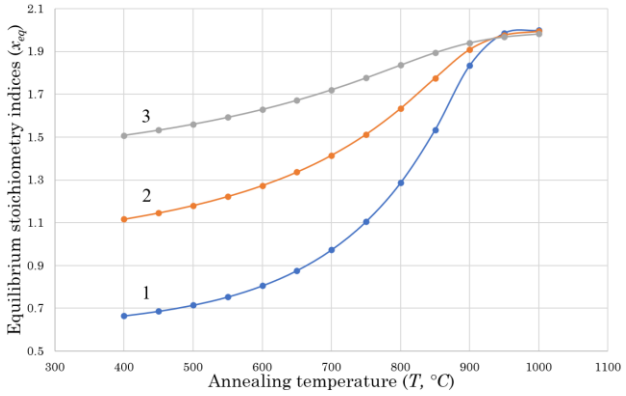

a

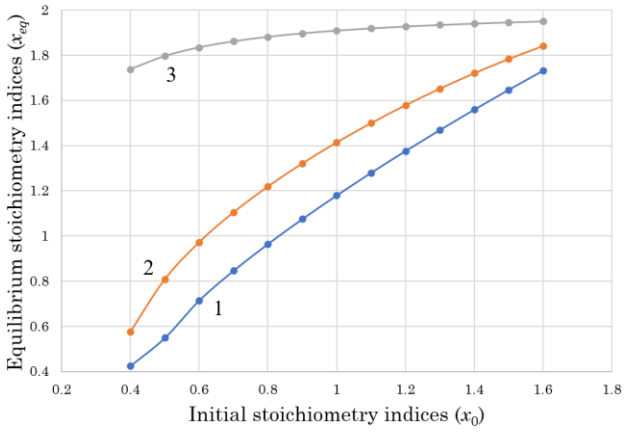

b

Fig. 2 – Equilibrium stoichiometry of Si oxide matrix versus annealing temperature at initial stoichiometry values, x_0: 1 – 0.6, 2 – 1, and 3 – 1.4 (a), versus initial stoichiometry at annealing temperatures, T: 1 – 500 °C, 2 – 700 °C, and 3 – 900 °C (b)

Fig. 2b shows the effect of the initial stoichiometry index of SiO$_x$ films on the equilibrium stoichiometry of Si oxide matrix for different annealing temperatures. As can be seen from this figure, all the dependences are increasing, defined by the functional form of the factor $(x - x_0)^2$ of the contribution of internal stress to the Gibbs free energy (2). It should be also noted that almost complete relaxation of the internal stress at a temperature of 900 °C leads to a very weak dependence of x_{eq} on x_0, much weaker compared to those at lower annealing temperatures.

3.2 Relative Amount of Si Precipitated in Si Phase

Fig. 3a shows the dependence of the relative amount of Si precipitated in the Si phase on the annealing temperature for different values of the initial SiO$_x$ stoichiometry. As can be seen from this figure, the precipitated Si fraction quickly increases with annealing temperature due to relaxation of internal stress and decrease in the corresponding contribution to the Gibbs free energy (2). Moreover, the graphs corresponding to different values of x_0 are quite close to each other and have an intersection point at a temperature of about 850 °C.

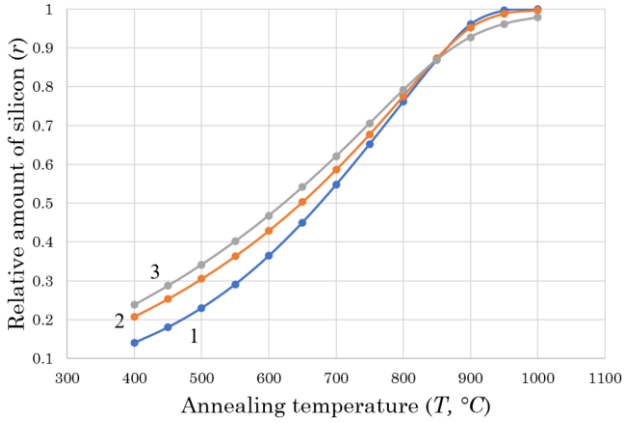

a

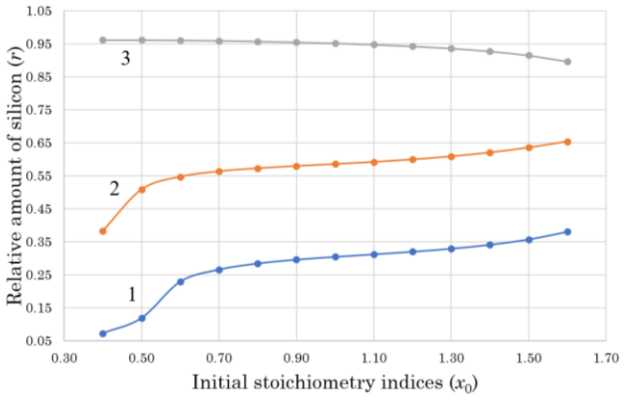

b

Fig. 3 – Relative amount of Si precipitated in the Si phase versus annealing temperature at initial stoichiometry values, x_0: 1 – 0.6, 2 – 1, and 3 – 1.4 (a), versus initial stoichiometry at temperatures, T: 1 – 500 °C, 2 – 700 °C, and 3 – 900 °C (b)

Fig. 3b shows the relative amount of separated Si versus initial SiO$_x$ stoichiometry for different annealing

temperatures. The data presented in this figure indicate that raise of the annealing temperature leads to ever slower growth of the function $r(x_0)$, which then changes to decrease at some temperature value below 900 °C. This may be explained by the fact that the main factor limiting the amount of the separated Si at lower temperatures is the internal stress in the phase-separated films. As the temperature grows, the internal stress mechanism begins to compete with the configuration entropy effect, which causes a descending dependence $r(x_0)$ (the equilibrium Si concentration in the Si oxide phase remains constant but the total Si concentration decreases with the increase in x_0. As demonstrated by Fig. 3a, equilibration of these mechanisms takes place at the temperature value of about 850 °C.

3.3 Size of Si Nanoparticles

Fig. 4a shows the evolution of the radius of Si nanoparticles at increasing the annealing temperature. As can be seen from this figure, all the dependences are practically linear up to a temperature of about 900 °C. After that, a transition to saturation occurs corresponding to saturation of the amount of separated Si (see Fig. 3a) due to almost complete relaxation of internal stress. The value of the Si particle radius is higher for larger excess Si content in the initial SiO_x films, which is obvious in view of that we consider a constant value of the Si nanoparticles concentration.

Fig. 4b shows the dependence of the radius of Si nanoparticles in the Si oxide matrix on the initial stoichiometry of the SiO_x film at different annealing temperatures. As can be seen from this figure, the dependences for the lower considered annealing temperatures change their character from ascending to descending at $x_0 = 0.5$ ($T = 700$ °C) and $x_0 = 0.6$ ($T = 500$ °C). These stoichiometry values correspond to a transition from a sharp to a slow increase in the respective dependences of the relative amount of Si precipitated in the Si phase on the initial stoichiometry index (see Fig. 3b). After this, the decrease of the nanoparticle size with an increase in the initial SiO_x stoichiometry is approximately linear, resulting from a decrease in the total amount of excess Si that can be separated into Si phase during phase separation process.

The peculiarities of the behavior of the dependences of the relative amount of separated Si and the Si nanoprecipitates radius at low values of x_0 and annealing temperatures may be explained as follows. At small values of x_0, the initial SiO_x phase contains large amounts of $Si - Si_4$ complexes with zero penalty energy and low contents of $Si - OSi_3$ and $Si - O_2Si_2$ complexes with the highest penalty energies. Therefore, the driving force for phase separation at such values of x is small and is easier balanced by both configuration entropy and internal stress mechanisms counteracting the separation process. The driving force increases with the increase in the value of x_0, which leads to the increase in both the amount of separated Si and the Si nanoparticles radius. Relaxation of the internal stress at raising the annealing temperature reduces the counteracting force to the phase separation thus shifting the transition point in the dependences shown in Fig. 4b to lower values of x_0.

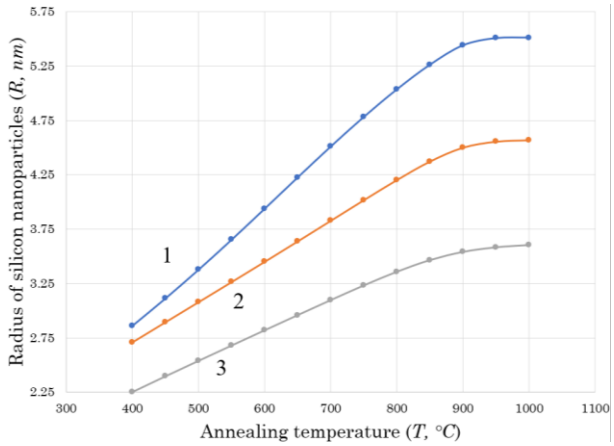

a

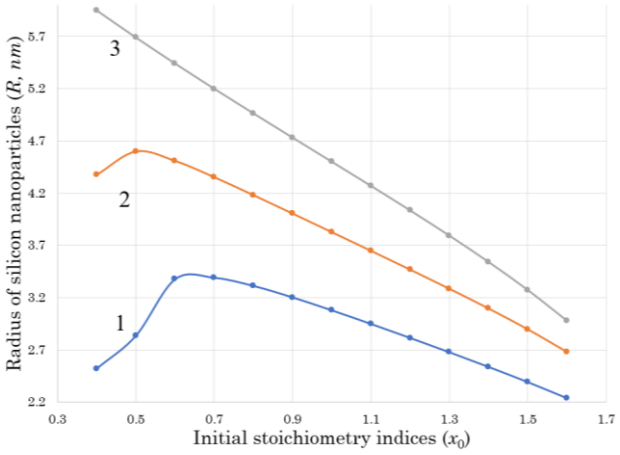

b

Fig. 4 – Radius of Si nanoparticles versus annealing temperature at initial stoichiometry values, x_0: 1 – 0.6, 2 – 1, and 3 – 1.4 (a), versus initial stoichiometry at annealing temperatures, T: 1 – 500 °C, 2 – 700 °C, and 3 – 900 °C (b)

3.4 Percolation Threshold

Fig. 5 shows the calculated dependence of the percolation threshold on the annealing temperature. Using the typical concentration of Si nanoinclusions formed during phase separation of nonstoichiometric Si oxides, $C_{incl} = 10^{18}$ cm^{-3}, the average distance between the nanoparticles was determined to be 10 nm, so that the calculations were performed for this particular nanoparticle diameter value. As can be seen from Fig. 5, the initial stoichiometry corresponding to the percolation threshold increases with annealing temperature and tends to saturation at T exceeding ~ 900 °C. This is due to the fact that with increasing temperature, an ever growing Si fraction is released as a result of internal stress relaxation, and, hence, an ever smaller excess Si concentration in the initial oxide is sufficient to form the nanoparticles, the diameter of which is equal to the distance between their centers. It should be noted as well that the dependence of the percolation threshold runs from approximately 750 °C, since at lower temperatures the amount of the separated Si at any initial oxide stoichiometry is insufficient to form particles with the sizes enabling their contact.

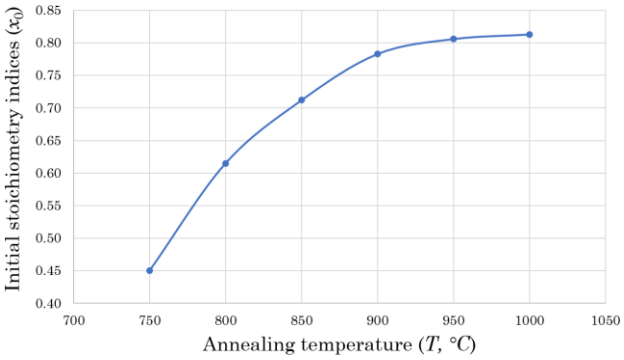

Fig. 5 – Temperature dependence of the percolation threshold

In [14], the percolation threshold between 0.5 and 0.7 in ultrathin SiO$_x$ films (4.5 nm) annealed at 1000 °C was determined experimentally. Later, the percolation threshold of about 0.7 for such films was confirmed by kinetic Monte Carlo simulations [15]. Taking into account simplicity of the model used here as well as neglecting the possible effects of the SiO$_x$ layer thickness on the morphology of the separated Si phase [25], the obtained value of 0.8 at 1000 °C (see Fig. 5) has a good correlation with the previously reported data.

4. CONCLUSION

In this work, the effect of annealing temperature and initial Si oxide stoichiometry in a wide range on the phase composition of Si/SiO$_x$ nanocomposites formed by phase separation of nonstoichiometric Si oxide films is studied by thermodynamic modeling. In particular, the equilibrium stoichiometry index of Si oxide matrix hosting Si nanoparticles, the relative amount of Si precipitated in the Si phase, and the average radius of Si nanoparticles in the phase separated Si/Si oxide composites as functions of annealing temperature are determined. The obtained functions are found to be ascending due to the relaxation of internal stress at increasing the temperature. At the annealing temperatures close to 900 °C, the equilibrium stoichiometry index of the Si oxide matrix approaches the stoichiometric value ($x = 2$) corresponding to complete phase separation, and the values of all the considered functions reach saturation.

It is found out that the effects of internal stress and configuration entropy lead to slightly ascending dependences of the relative amount of Si separated in the Si phase, on the initial SiO$_x$ stoichiometry at the temperatures below a threshold value of about 850 °C. These dependences change to slightly descending ones above this threshold due to complete stress relaxation. Moreover, the relative amount of Si precipitated in the Si phase as well as the Si nanoparticles radius grow fast at smaller x0 values, which is caused by small values of the contribution of the penalty energy of Si–O$_y$Si$_{4-y}$ structural units to the Gibbs free energy. At higher x_0 values, the Si nanoparticles radius linearly decreases due to the decrease in the excess Si concentrations in the initial SiO$_x$ films.

A non-zero percolation threshold value is achieved beginning from ~ 750 °C, at which sufficient amount of excess Si may be released to form nanoparticles with the diameters coinciding with the distance between them. The percolation threshold is an ascending function of the annealing temperature, which is explained by ever larger amount of separated Si due to internal stress relaxation.

The obtained results have a scientific and practical significance. In particular, they may be used for creating Si/Si oxide nanocomposites with tailored properties for nanoelectronic device applications.

REFERENCES

1. G. Hassand, C.D. Salzberg, *J. Opt. Soc.* **44**, 181 (1954) https://doi.org/10.1364/JOSA.44.000181.
2. *The Physics and Chemistry of SiO₂ and the Si–SiO₂ Interface* (Eds. by C.R. Helms, B.E. Deal) (New York: Plenum: 1988) https://doi.org/10.1007/978-1-4899-0774-5.
3. J. Michael, J. O'Leary, H. Thomas, *J. Vac. Sci. Technol. A.* **5** No 1, 106 (1987) https://doi.org/10.1116/1.574142.
4. R.F. Steimle, R. Muralidhar, R. Rao, M. Sadd, C.T. Swift, J. Yater, B. Hradsky, S. Straub, H. Gasquet, L. Vishnubhotla, E.J. Prinz, T. Merchant, B. Acred, K. Chang, B.E. White, *Microelectron. Reliab.* **47** No 4-5, 585 (2007) https://doi.org/10.1016/j.microrel.2007.01.047.
5. A.S. Kale, W. Nemeth, H. Guthrey, E. Kennedy, A.G. Norman, M. Page, M. Al-Jassim, D.L. Young, S. Agarwal, P. Stradins, *Appl. Phys. Lett.* **114** No 8, 083902 (2019) https://doi.org/10.1063/1.5081832.
6. M. Wang, A. Anopchenko, A. Marconi, E. Moser, S. Prezioso, L. Pavesi, G. Pucker, P. Bellutti, L. Vanzetti, *Physica E* **41**, 912 (2009) https://doi.org/10.1016/j.physe.2008.08.009.
7. Z. Yu, M. Aceves-Mijares, *Appl. Phys. Lett.* **95**, 081101 (2009) https://doi.org/10.1063/1.3210784.
8. I.P. Lisovskyi, A.V. Sarikov, M.I. Sypko, *Thin-Film Structures with Si Nanoinclusions. Physics, Technology, Perspective Applications* (Kyiv – Chernivtsi: Knyhy–XXI: 2014) [in Ukrainian].
9. A. Sarikov, M. Zacharias, *J. Phys.: Condens. Matter* **24** No 38, 385403 (2012) https://doi.org/10.1088/0953-8984/24/38/385403.
10. A. Sarikov, *Nanomanufacturing* **3**, 293 (2023) https://doi.org/10.3390/nanomanufacturing3030019.
11. V.A. Dan'ko, I.Z. Indutnyi, V.S. Lysenko, I.Y. Maidanchuk, V.I. Min'ko, A.N. Nazarov, A.S. Tkachenko, P.E. Shepelyavyi, *Semiconductors* **39**, 1197 (2005) https://doi.org/10.1134/1.2085270.
12. D.M. Zhigunov; V.N. Seminogov, V.Y. Timoshenko, V.I. Sokolov, V.N. Glebov, A.M. Malyutin, N.E. Maslova, O.A. Shalygina, S.A. Dyakov, A.S. Akhmanov, V.Ya. Panchenko, P.K. Kashkarov, *Physica E* **41**, 1006 (2009) https://doi.org/10.1016/j.physe.2008.08.026.
13. A. Sarikov, *Solid State Commun.* **179**, 39 (2014) https://doi.org/10.1016/j.ssc.2013.11.016.
14. J. Laube, S. Gutsch, D. Hiller, M. Bruns, C. Kübel, C. Weiss, M. Zacharias, *J. Appl. Phys.* **116**, 223501 (2014) https://doi.org/10.1063/1.4904053.
15. A. Sarikov, M. Semenenko, S. Shahan, *CrystEngComm* **26**, 2836 (2024) https://doi.org/10.1039/D4CE00212A.
16. A. Bongiorno, A. Pasquarello, *Phys. Rev. B.* **62** No 24, R16326 (2000) https://doi.org/10.1103/PhysRevB.62.R16326.
17. A. Sarikov, V. Litovchenko, I. Lisovskyy, I. Maidanchuk, S. Zlobin, *Appl. Phys. Lett.* **91**, 133109 (2007) https://doi.org/10.1063/1.2790814.
18. E.P. Donovan, F. Spaepen, J.M. Poate, D.C. Jacobson, *Appl. Phys. Lett.* **55** No 15, 1516 (1989) https://doi.org/10.1063/1.101593.

19. C. Spinella, S. Lombardo, F. Priolo, *J. Appl. Phys.* **84** No 10, 5383 (1998) https://doi.org/10.1063/1.368873.
20. O. Nast, *The Aluminium-Induced Layer Exchange Forming Polycrystalline Silicon on Glass for Thin-Film Solar Cells*. Ph.D. Thesis, Philipps-Universität Marburg, Marburg, Germany (2000) https://archiv.ub.uni-marburg.de/diss/z2000/0423/pdf/don.pdf.
21. K. Winer, *Phys. Rev. B* **41**, 12150 (1990) https://doi.org/10.1103/PhysRevB.41.12150.
22. A. La Magna, G. Nicotra, C. Bongiorno, C. Spinella, G.M. Grimaldi, E. Rimini, L. Caristia, S. Coffa, *Appl. Phys. Lett.* **90** No 18, 183101 (2007) https://doi.org/10.1063/1.2734398.
23. S. Boninelli, F. Iacona, G. Franzò, C. Bongiorno, C. Spinella, F. Priolo, *J. Phys.-Condens. Mat.* **19** No 22, 225003 (2007) https://doi.org/10.1088/0953-8984/19/22/225003.
24. M. Roussel, E. Talbot, P. Pareige, F. Gourbilleau, *J. Appl. Phys.* **113**, 063519 (2013) https://doi.org/10.1063/1.4792218.
25. D.J. Seol, S.Y. Hu, Y.L. Li, J. Shen, K.H. Oh, L.Q. Chen, *Acta Mater.* **51**, 5173 (2003) https://doi.org/10.1016/S1359-6454(03)00378-1.

Термодинамічне моделювання фазового складу структур Si/SiO$_x$, отримуваних фазовим розділенням нестехіометричних оксидів кремнію

В. Наголенко[1], А. Саріков[2,3,4], О. Рижко[1]

[1] *«Науковий ліцей імені Анатолія Лигуна» Кам'янської міської ради Дніпропетровської області, 51925 Кам'янське, Україна*
[2] *Інститут фізики напівпровідників імені В. Є. Лашкарьова Національної академії наук України, 03028 Київ, Україна*
[3] *Інститут високих технологій Київського національного університету імені Тараса Шевченка, 03022 Київ, Україна*
[4] *Національний технічний університет України «Київський політехнічний інститут імені Ігоря Сікорського», 03056 Київ, Україна*

У статті досліджено вплив температури відпалу та початкової стехіометрії оксиду кремнію в широких діапазонах на фазовий склад нанокомпозитів Si/SiO$_x$, отримуваних фазовим розділенням при високотемпературних відпалах. У цьому дослідженні враховано появу механічних напружень, що перешкоджають процесу фазового розділення. В рамках термодинамічного підходу промодельовано залежність від зазначених параметрів рівноважної стехіометрії матриці оксиду кремнію, відносної кількості кремнію, виділеного у кремнієву фазу, та середнього розміру частинок кремнію. Визначено залежність порогу перколяції кремнієвих нановключень від температури відпалу. Отримані результати проаналізовано, порівнюючи внески різних механізмів у вільну енергію систем кремній/оксид кремнію під час фазового розділення.

Ключові слова: Нестехіометричний оксид кремнію, Фазовий склад, Фазове розділення, Нановключення кремнію, Поріг перколяції.